

Experimental demonstration of a left-handed metamaterial operating at 100 GHz

M. Gokkavas,^{1,*} K. Guven,¹ I. Bulu,¹ K. Aydin,¹ R. S. Penciu,³ M. Kafesaki,³ C. M. Soukoulis,^{3,4} and E. Ozbay^{1,2}

¹Department of Physics, Bilkent University, Bilkent, 06800 Ankara, Turkey

²Nanotechnology Research Center, Bilkent University, Bilkent, 06800, Ankara, Turkey

³Institute of Electronic Structure and Laser, Foundation for Research and Technology, Hellas & Dept. of Materials Science and Technology, University of Crete, Greece

⁴Ames Laboratory-USDOE and Department of Physics and Astronomy, Iowa State University, Ames, Iowa 50011

Abstract

The existence of a left-handed (LH) transmission peak in a bulk composite metamaterial (CMM) at around 100 GHz is demonstrated experimentally. The metamaterial consists of stacked planar glass layers on which periodic patterns of micron-scale metallic wires and splitting resonators (SRRs) are fabricated. The left-handed nature of the CMM peak is proved experimentally by comparing the transmission spectra of the various CMM components. Theoretical investigation of the system, including transmission calculations and an inversion scheme for the retrieval of the effective permeability and permittivity of the system, further supports the existence of negative refraction.

* Correspondence and requests for materials should be addressed to M. Gokkavas (e-mail: mgokkavas@fen.bilkent.edu.tr).

The idea of left-handed (LH) materials, i.e. materials with both negative electrical permittivity (ϵ) and magnetic permeability (μ), where the electric field (\mathbf{E}), magnetic field (\mathbf{B}), and wave vector (\mathbf{k}) form a left-handed coordinate system, was developed by Veselago (1) decades ago. However, it was only recently that such materials were investigated experimentally (2, 3), despite their rich physics and the large number of associated potential applications (4), e.g. in the formation of a perfect lens (5). The first experimental realization of LH-materials was achieved by separately constructing $\epsilon < 0$ and $\mu < 0$ components, and then by combining them together forming a composite metamaterial (CMM). Although it has been well known how to obtain a $\epsilon < 0$ material easily (e.g. using wire arrays (6)), the realization of $\mu < 0$ response (especially at high frequencies) has been a challenge, due to the absence of naturally occurring magnetic materials with negative μ . The possibility of the realization of a $\mu < 0$ material was predicted in 1999 by Pendry et al., who suggested a design made of concentric metallic rings with gaps, called split ring resonators (SRRs) which exhibits a $\mu < 0$ regime in the vicinity of the magnetic resonance frequency ω_m of the SRR structure (7). Using arrays of SRRs and wires, different designs and configurations of CMMs are reported. (2, 3, 8)

CMMs are usually fabricated as periodic structures; the periodicity in the two directions is achieved by printing 2D-arrays of metallic patterns on planar substrates, whereas the periodicity in the third direction is achieved by stacking a large number of such patterned planar substrates. The use of a stack of planar substrates has been common to all CMMs reported up to date.

The fabrication of CMMs for infrared and optical frequencies necessitates higher resolution photolithography as well as thinner substrates, or even the use of a single substrate coupled with multilayer processing in the case of extremely small dimensions as required for optical frequencies. Up to date, the highest reported frequency for $\mu < 0$ response in a SRR-only medium has been 100 THz; the relevant medium was composed of e-beam patterned SRRs on a single substrate layer, and the $\mu < 0$ response was

demonstrated using excitation with propagation vector perpendicular to the SRRs-plane (9). This monolayer approach (9, 10) works fine for SRR-only structures, since the periodicity of SRRs in the direction perpendicular to their plane is not essential for the demonstration of the existence of a magnetic resonance. The only multilayer SRR-only medium with a THz magnetic resonance reported up to date was obtained by a multilayer microfabrication process, in which a few layers of 2D-SRR arrays separated by polyimide coating were fabricated on a single substrate (11). However, for the demonstration of LH behavior (i.e. both $\epsilon < 0$ and $\mu < 0$ response) in a CMM, where the periodicity in the stacking direction is crucial, the multilayer-single-substrate technology is extremely difficult to implement, since one needs tens of layers (to achieve a thickness comparable to the operation wavelength). Recently, Moser et al. reported a transmission peak at 2.5 THz from a CMM-type material measured by Fourier Transform Infrared Spectroscopy (12). Their results were obtained from a monolayer of in-plane SRR and wire arrays (i.e. wires next to the SRRs) under normal incidence. Although this was a proof of concept demonstration for one layer CMM, the lack of multi-layer CMM structure prevented the demonstration of true left handed propagation of electromagnetic (EM) waves. This demonstration is possible only when the magnetic resonance is excited by the magnetic field (as opposed to excitation by the electric field such as in (12)), which implies propagation direction parallel to the SRR-wire planes (this is the only way for the SRRs to respond as a $\mu < 0$ material (13)).

Notice that the work at THz region regime shows only a negative μ and not a negative n (13). In this letter, we report the smallest multilayer-CMM fabricated to date, which exhibits a LH transmission peak at 100 GHz and a negative index of refraction in this frequency range. The 100 GHz LH peak reported in this work corresponds to a 10-fold increase in frequency compared to previous work (2). Although the scalability assists us to project the available structures to different operation frequencies across the electromagnetic spectrum, a refined approach is needed when the characteristic length scale of the structure starts to become comparable to electrodynamic interaction scales.

In particular, the skin depth, δ , of the metal and the distribution of the local fields and currents induced by the propagating electromagnetic field need to be analyzed carefully. For typical fabrication metals (Aluminium, Gold, Copper, and Silver) $\delta \sim 0.25 \mu\text{m}$ at $f \sim 100$ GHz which is already a comparable value. Unfortunately, the current and field distributions are quite complicated and depend on both the material and the geometrical parameters of the structure and the substrate. Lack of simple but precise formulas for determining the resonance frequency of SRRs necessitates the use of extensive numerical calculations. The dielectric substrate generates a non-uniform distribution of the local field of SRRs, [17] which then affects the capacitive-inductive (LC) response of the SRR, hence its resonance frequency.

On the other hand, limitations in the practical realization of CMM restricts the applicability of a mere geometrical scaling. In particular, the thickness of the substrate layer is a constraint. We used standard 22 mm x 22 mm x 150 μm layers of Corning glass as the substrate. This thickness ensures structural rigidity and the air gap between the layers present in the microwave structures is eliminated.

The challenging task is to design the wire-only medium subject to the predetermined periodicity by SRR geometry and substrate thickness, with a plasma frequency ω_p , high above the magnetic resonance frequency of SRRs, ω_m . The actual ω_p of the CMM is *lower* than that of its wire-only component, due to the electric response of SRRs. (8, 14) This can be verified by employing a CMM consisting of CRRs + wires, since the CRR bears the same electric response as the SRR. Hence, one has to ensure that the ω_p of the CMM remains above ω_m for the existence of a left-handed transmission band. This, in turn, requires a high ω_p of wire-only medium to start with.

Pendry *et al.* formulated the low frequency plasmons in metallic mesostructures by relating the microscopic quantities (effective electron density, n_{eff} , and effective electron mass, m_{eff}) to the macroscopic parameters of the system (wire radius, r and the periodicity of the lattice, a) through the plasma frequency,

$$\omega_p^2 = \frac{n_{\text{eff}} e^2}{\epsilon_0 m_{\text{eff}}} = \frac{2\pi c_0^2}{a^2 \ln(a/r)}. \quad (1)$$

This expression provides a very clear description of the physics of the plasmon in terms of the design parameters of the structure. At fixed periodicity, the only possibility appears to be the increase in the wire radius for increasing ω_p . However, this yields only a marginal increase,

$$\frac{\omega_p'}{\omega_p} = \sqrt{\frac{\ln(r/a)}{\ln(r'/a)}}, \quad (r < a/2, r' < a/2)$$

since in this case *both* n_{eff} and m_{eff} acquires an enhancement. The catch here is that the formula describes the plasma frequency in terms of a *single* wire element in the unit cell. We relax this condition by letting the unit cell to accommodate multiple parallel wires. In this case, the m_{eff} would roughly be the same (since the wire radius did not change) but n_{eff} is multiplied by the number of wires, n , in the unit cell. This gives a \sqrt{n} -fold increase in the plasma frequency. Note that this design implies less absorption compared to that of the single wire designed for the same ω_p , as well.

Figure 1(a) and (b) show one unit cell of the SRR and the wire micropatterns, respectively. The unit cell contains one SRR, and two layers of triple wire pattern. Employing two consecutive wire layers increases the coupling and the overall density of wires, which shifts ω_p , (edge of the $\epsilon < 0$ stop band) further higher. The dimensions of the components are as follows: Inner ring inner radius: $r_{ii} = 43 \mu\text{m}$, inner ring outer radius: $r_{io} = 67.2 \mu\text{m}$, outer ring inner radius: $r_{oi} = 80.7 \mu\text{m}$, outer ring outer radius: $r_{oo} = 107.5 \mu\text{m}$, split ring gap: $d = 7.2 \mu\text{m}$, wire width: $w = 26.9 \mu\text{m}$, wire separation: $d_w = 53.7 \mu\text{m}$. The periodicity in x - and y -directions is $a_x = a_y = 262.7 \mu\text{m}$.

The metamaterial pattern is printed on glass substrates by employing UV-photolithography followed by microfabrication with a metal thickness of 100 Å Ti /

4500 Å Au. SRRs, CRRs, and wire layers were fabricated separately, and then stacked for measurements. For SRR-only, CRR-only and wire-only stacks, plain glass layers were used as spacers, so that the resulting periodicity of the components is the same as in the final CMM structure. The number of unit cells in the propagation direction is 10 for all structures.. The final CMM was composed of 100 layers, having a 15 mm (100 x 150 μm) width (z), 20 mm height (y), and 2.6 mm length (x), x being the propagation direction. Figure 1(c) shows the schematic of the CMM, while Fig. 2 is a photomicrograph of one SRR-layer and stacked on top of one wire-layer. The patterns were aligned to the glass substrate edge during photolithography, hence the alignment within the resulting metamaterial structure is limited by the edge uniformity of the substrates.

The transmission spectrum was measured by a millimetre wave network analyzer. Figure 3 shows the normal-to-the-plane transmission spectrum of SRR-only for two different SRR orientations. In this configuration, the magnetic resonance can be excited only through the electric field (13), when the SRR is asymmetric with respect to \mathbf{E} . Since the asymmetric orientation causes a misbalance of the charge distribution and induces circulating currents on SRRs; the result is a resonant electric response of the system, which appears as a gap. On the other hand, the symmetric orientation with respect to \mathbf{E} is transparent. Increasing the number of layers enhances and, due to interlayer coupling between SRRs, widens the resonance gap.

We systematically investigated the transmission spectra of wire, SRR, CRR, and CMM structures to show that the transmission band of CMM appears in the common frequency range of the the $\epsilon < 0$ stop band of wires (modified by the SRR presence (14)) and the $\mu < 0$ stop band of SRRs (8). Figure 4 shows that the $\epsilon < 0$ stop-band of the wire-only structure extends across the entire W-band. The onset of transmission above 118 GHz signals the ω_p of wires. The CRR-only structure is transparent in this regime,

since it is non resonant. In contrast, the SRR-only structure exhibits a clear resonance ($\mu < 0$) between 95-108 GHz with -30 dB minimum occurring at 102 GHz.

In order to contrast the CMM response, a “non-working” CMM is made by replacing SRR layers with CRR layers. Figure 5 shows the transmission spectra of CMM structures incorporating SRRs, and CRRs, respectively. The SRR-only spectrum is indicated by dotted lines. Evidently, the CMM structure exhibits a pass band between 96 GHz to 107 GHz with a -25 dB maximum at 101 GHz. We stress that this band matches the $\mu < 0$ stop band of SRRs. On the other hand, the CMM incorporating CRR layers remains opaque throughout the frequency range. As a result, we conclude that the pass band of CMM indicates truly a left-handed behaviour.

We have also studied our structures theoretically, performing transmission calculations (using the Finite Integration Technique, employed through the commercial MicroWave Studio program) and applying a retrieval procedure (15) to obtain the effective material parameters from the transmission and reflection data. Figure 6 shows the transmission properties obtained from these simulations. The magnetic resonance of the SRR-only structure extends from 96 GHz to 107 GHz which exactly coincides with the magnetic resonance obtained from the experiments. The calculated ω_p for the wire-only structure is above 150 GHz. The CMM structure exhibits a transmission band from 98 to 104 GHz, with a peak transmission of -14 dB. The retrieval procedure yields an effective refractive index of -5.2 from 98 to 104 GHz. The difference between theory and experiment in terms of the transmission level arises due to the following reasons. (i) The loss of metal and substrate are included by reference conductance values, and the finite thickness (in relation to skin depth) is not considered theoretically. (ii) The substrate length along the propagation direction is different: the substrate is of the CMM size (2.6 mm) in the simulation, but 22 mm long in the experiment. The simulation size is kept intentionally small to provide a high resolution computational mesh for handling small features of SRRs and wires, in trade of a certain mismatch in the loss. Note however,

that this does not affect the spectral distribution of the response. (iii) Experimental disorder and misalignment degrades the transmission significantly, as reported in a recent study.[16] Fabrication-based nonuniformity of SRR and wire elements (especially close to the mask edges), and misalignment induced by variations in substrate size are inherent problems. In contrast, the simulation relies on the ordered and periodic nature of the structure. Therefore, a fair comparison between theory and experiment in terms of transmission level is not available at present.

In conclusion, we have successfully demonstrated the left-handed behaviour in the smallest multilayer SRR + wire type CMM reported up to now. The CMM was fabricated on glass-substrates, using photolithography and microfabrication procedures, and demonstrated a left-handed transmission peak at ~ 100 GHz. The left-handed transmission band exactly coincided with the stop-band of the SRR-only medium; it was below the cut-off frequency of the electric response of the system, and disappeared when the splits of the SRRs were shorted, proving unambiguously the left-handed nature of the measured peak. The left-handed nature of the peak was further proved by theoretical simulations.

Acknowledgements

This work was supported by the projects EU-DALHM, EU-NOE-METAMORPHOSE, EU-NOE-PHOREMOST, TUBITAK-104E090, DARPA-HR0011-05-C-0068, Greek Ministry of Education PYTHAGORAS and by Ames Laboratory (Contract No. W-7405-Eng-82). E. Ozbay acknowledges partial support from the Turkish Academy of Sciences. The research of C. M. Soukoulis is further supported by the Alexander von Humboldt senior-scientist award 2002.

References

1. V. G. Veselago, *Sov. Phys. Usp.* **10**, 504 (1968).

2. D.R. Smith, W.J. Padilla, D.C. Vier, S.C. Nemat-Nasser, and S.Schultz, Phys. Rev. Lett. **84**, 4184 (2000).
3. R.A. Shelby, D.R. Smith, S.C. Nemat-Nasser, and S.Schultz, Apl. Phys. Lett. **78**, 480 (2001).
4. N. Engheta, R.W. Ziolkowski, IEEE Tran. Microw. Theory Tech. **53**, 1535 (2005).
5. J.B. Pendry, Phys. Rev. Lett. **85**, 3966 (2000).
6. J.B. Pendry, A.J. Holden, W.J. Stewart, and I. Youngs, Phys. Rev. Lett. **76**, 4773 (1996).
7. J.B. Pendry, A.J. Holden, D.J. Robbins, and W.J. Stewart, IEEE Trans. Microwave Theory Tech. **47**, 2075 (1999).
8. K. Aydin, K. Guven, M. Kafesaki, L. Zhang, C. M. Soukoulis, and E. Ozbay, Opt. Lett. **29**, 2623 (2004).
9. S. Linden, C. Enkrich, M. Wegener, J. Zhou, T. Koschny, and C. M. Soukoulis, Science **306**, 1351 (2004).
10. T.J. Yen, W.J. Padilla, N. Fang, D.C. Vier, D.R. Smith, J.B. Pendry, D.N. Basov, and X. Zhang, Science **303**,1494 (2004).
11. N. Katsarakis, G. Konstantinidis, A.Kostopoulos, R.S. Penciu, T.F. Gundogdu, M. Kafesaki, E.N. Economou, T. Koschny, and C. M. Soukoulis, Opt. Lett. **30**, 1348 (2005).
12. H.O. Moser, B.D.F. Casse, O. Wilhelmi, and B.T. Saw, Phys. Rev. Lett. **94**, 063901 (2005).
13. N. Katsarakis, T. Koschny, M. Kafesaki, E. N. Economou and C. M. Soukoulis, Appl. Phys. Lett. **84**, 2943 (2004).
14. T. Koschny, M. Kafesaki, E. N. Economou, and C. M. Soukoulis, Phys. Rev. Lett. **93**, 107402 (2004).
15. D. R. Smith, D. C. Vier, T. Koschny, and C. M. Soukoulis, Phys. Rev. E **71**, 121103 (2005).

16. K. Aydin, K. Guven, N. Katsarakis, C. M. Soukoulis, and E. Ozbay, *Opt. Exp.* **12**, 5896 (2004).
17. M. Kafesaki, T. Koschny, R. S. Penciu, T. F. Gundogdu, E. N. Economou, and C. M. Soukoulis, *J. Opt. A* **7**, S12 (2005).

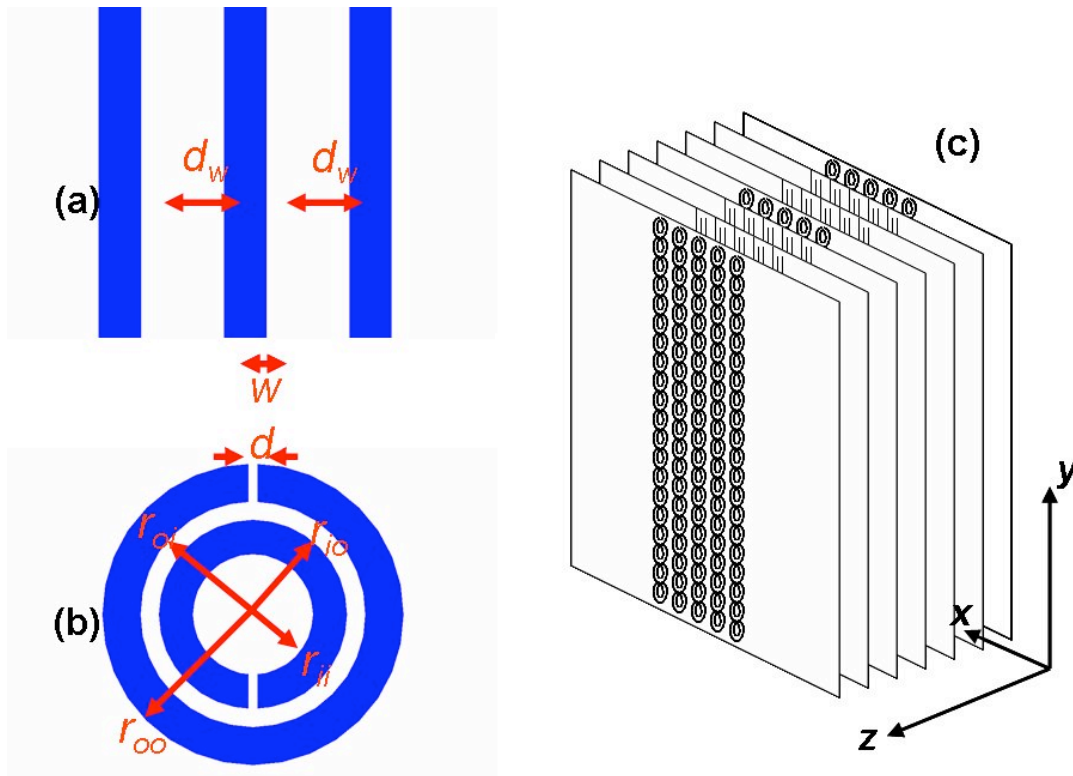


Fig. 1: (a) Wire geometry employed for the mm-wave CMM. (b) SRR geometry employed for the mm-wave (CMM). (c) Schematic geometry of the CMM, consisting of periodically stacked (along z-direction) two layers of wire-patterned substrates and one layer of SRR-patterned substrate.

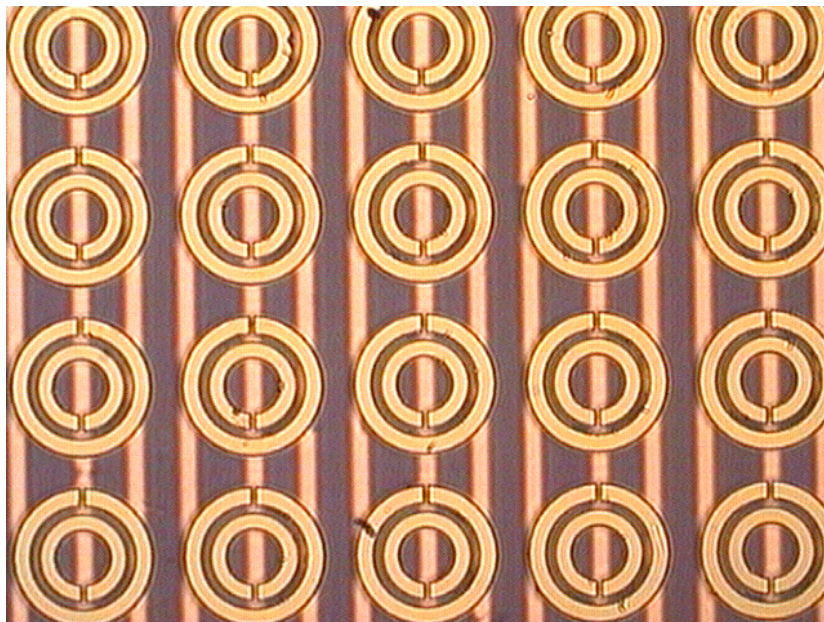


Fig. 2: Photomicrograph showing the mm-wave CMM sample. No special alignment procedure using the microscope was performed for this picture. The two patterns were aligned by aligning the edges of the glass substrates.

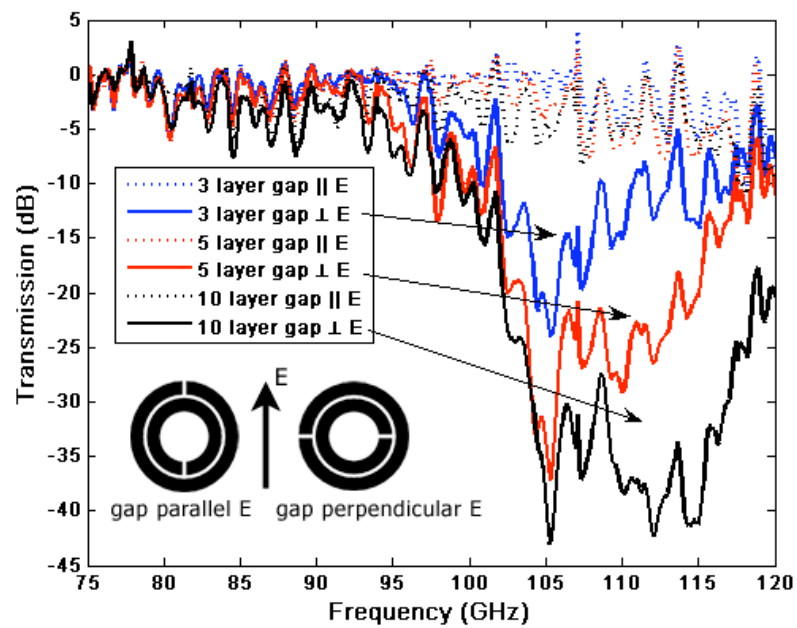


FIG. 3 (Color online) Transmission spectra of the SRR-only structure for propagation normal to the SRR plane: SRR-splits parallel to E (dotted) and perpendicular to E (solid). Electric coupling to the magnetic resonance occurs in the latter case.

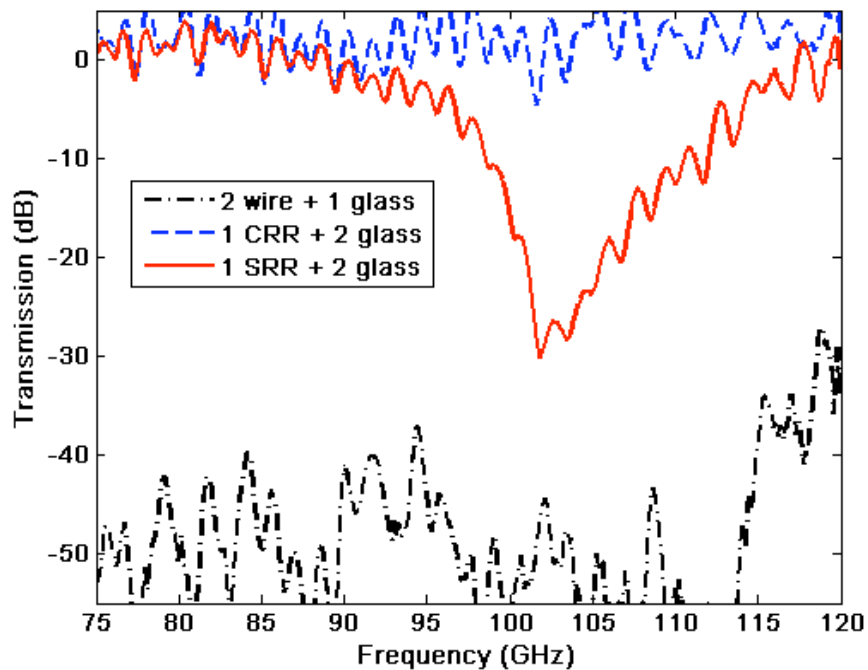


Fig. 4: (color online) Transmission spectra of wire (dash-dotted), CRR (dashed), and SRR (solid) structures.

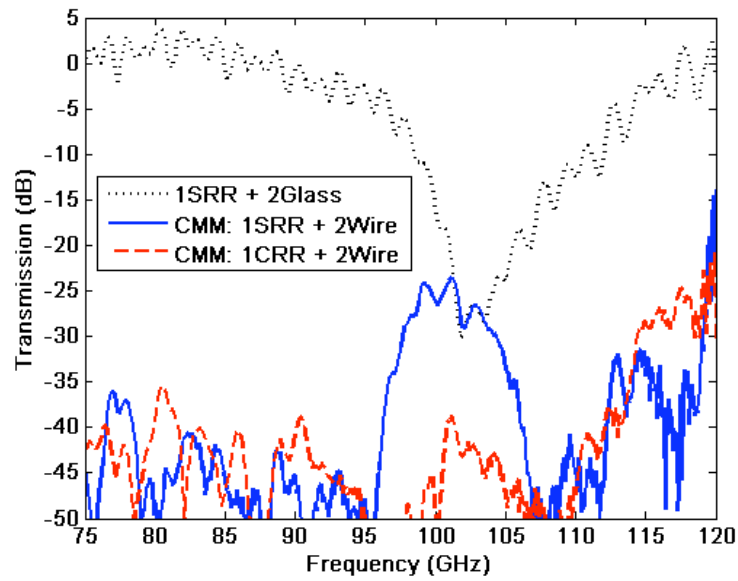


Fig. 5: (color online) Transmission spectra of CMM (SRR+wire) (solid), Closed-CMM (CRR+wire) (dashed) and SRR-only structures (dotted). The SRR-only spectrum is shown to compare left-handed transmission band and negative permittivity gap.

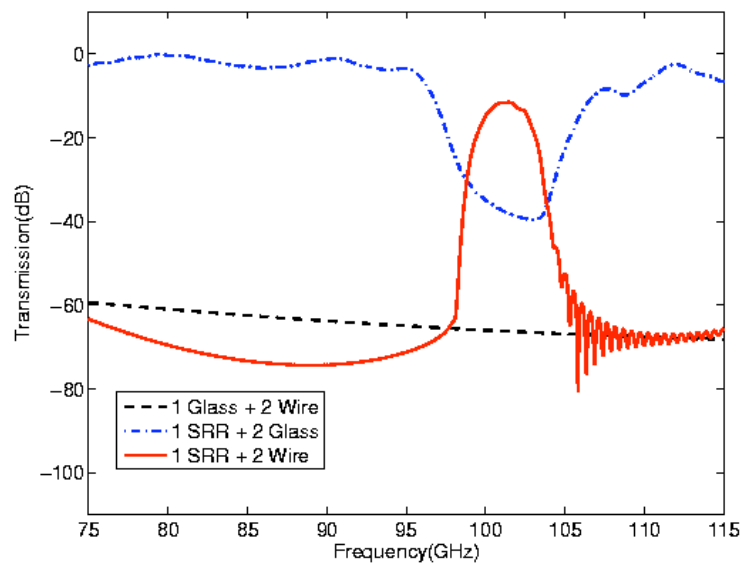


Fig.6: Theoretical simulations for the transmission spectrum of CMM (solid-red), SRR-only (blue-dot-dashed), and wire-only (dashed) structures for 10 unit cells in the propagation direction.